Geometric Approach to Fault Detection and Isolation in Multivariate Structural Systems: An Experimental Investigation

N. Rahimi[1]
Mech. Eng. Group
School of Eng.
Imam Hossein Univ.

M.H. Sadeghi[2]
Mech. Eng. Dep't.
School of Eng.
Tabriz Univ.

M.J. Mahjoob[3]
Mech. Eng. Dep't.
Tehran Univ.

ABSTRACT

In this paper, fault isolation of a laboratory scale structural frame, as a multivariate system, has been investigated, using a geometric approach in conjunction with parametric system identification. The proposed geometric approach is based on the assumption that each fault mode may be regarded as a hyper-surface in an appropriate topological space, where the hyper-surfaces are constructed based on the estimated parameters. Finally, by defining proper metric and assuming the unknown mode (of a system) being as a point in space, where the estimated parameters are the coordinates, the fault mode can be identified by minimizing the obtained distances between the point and each of the hyper-surfaces. Based on the number of inputs and measured outputs, the frame was modeled by standard ARX and VARX models in four different forms as Single-Input Single-Output (SISO), Single-Input Multiple-Output (MISO), Single-Input Multiple-Output (SIMO) and Multiple-Input Multiple-Output (MIMO). Also, the performance of the scheme was evaluated in deterministic and probabilistic spaces. The obtained results revealed that the MIMO representation of the frame in the probabilistic space had an acceptable performance which was the highest in comparison with the others and the SISO representation system in the deterministic space had the lowest performance.

Key Words: Fault Isolation, Multivariate Systems, Structural Systems, Parametric Estimation, Geometric Approach

آشکارسازی و جداسازی عیب به روش هندسی درسیستم‌های سازه‌ای با ورودی و خروجی‌های چندگانه- بررسی تجربی

ناصر رحیمی
گروه مهندسی مکانیک
دانشکده فنی و مهندسی
دانشگاه امام حسین(ع)

مرتضی همایون صادقی
گروه مهندسی مکانیک
دانشکده فنی و مهندسی
دانشگاه تبریز

محمد محجوب جهرمی
دانشکدهٔ مهندسی مکانیک
دانشگاه تهران

(تاریخ دریافت: ۱۳۸۷/۰۲/۰۲، تاریخ پذیرش: ۱۳۸۸/۰۴/۱۵)

چکیده

در این مقاله، گزارش و نتایج حاصل از جداسازی عیب (شناسایی نوع) به روش هندسی در یک قاب فولادی ارائه و اعتباربخشی روش مذکور برای عیب‌یابی سیستم‌های دینامیکی دارای ورودی و خروجی‌های چندگانه انجام شده است. در روش هندسی که یکی از روش‌های عیب‌یابی مبتنی بر مدل است، مدل‌سازی با استفاده از روش‌های پارامتری شناسایی سیستم انجام می‌شود. برای مدل‌سازی قاب مورد نظر از مدل‌های پارامتری ARX وVARX با تعداد ۸ پارامتر استفاده شده است. عیب‌یابی قاب یادشده به صورت سیستم‌های یک ورودی-یک‌خروجی(SISO) ، یک ورودی-دو خروجی(SIMO)، دو ورودی-یک‌خروجی(MISO) و دو ورودی-دو خروجی(MIMO) در دو فضای معین و احتمالی انجام شده و مقایسه نتایج صورت گرفته است. نتایج عیب‌یابی قاب مزبور به صورت سیستم MIMO و در فضای احتمالی از دقت موردقبول برخوردار بوده، بالاترین دقت را دارد و پایین‌ترین دقت مربوط به سیستم SISO و در فضای معین می‌باشد.

واژه‌های کلیدی: جداسازی عیب، سیستم‌های چندورودی-چندخروجی، سیستم‌های سازه‌ای، شناسایی پارامتری سیستم، روش هندسی

1-PhD Graduate (Corresponding Author): nrahimi@ihu.ac.ir
2-Associate Professor: morteza@tabrizu.ac.ir
3-Associate Professor: mmahjoob@ut.ac.ir

1. Introduction

Fault diagnosis methods are generally classified in two categories: System-Based and Model-Based methods. System-Based methods consist mainly of Hardware Redundancy (Voting) [1-2], Software Redundancy [3-4] and Fault-Sensitive-Filter methods[5-7] and despite being used easily, they have major limitations and drawbacks which are: 1) requiring detailed mathematical models (usually in the state space form) of the process; 2) being suitable for sensor and actuator fault detection, and are not, in general, applicable for system faults; 3) being suitable for the deterministic case and suboptimal in the presence of the noise[8].
Model-Based methods mainly consist of Multiple Model [9-11], Parametric Modeling [12-14] and Nearest Neighbor [15] methods which do not have the above mentioned limitations and drawbacks, but the major disadvantage of these methods is their failur if the operational mode is not exactly the same as any of the pre-modeled modes.

Geometric approach in fault diagnosis does not have the mentioned limitation and has been employed for different systems; However, only the SISO systems have been investigated [16-18]. Recently, the geometric approach was modified and improved to cope with the MIMO systems [19-20]. In this paper, an experimental investigation of the geometric approach to fault isolation has been carried out for a laboratory-scale steel frame structure. Based on the number of the inputs and measured outputs, the frame was modeled in four different types including SISO, MISO, SIMO, and MIMO systems.

In fault diagnosis by the geometric approach, each of the faulty modes are modeled as a hyper-surface, and each hyper-surface is constructed by using a group of feature vectors associated with a specific faulty mode, where these feature vectors are obtained by the parametric system identification method. Each feature vector is a point and each hyper-surface is a subspace in *n*-dimensional configuration space.

Fault diagnosis is achieved by calculating distances of the feature vector of an unknown operational mode with each of the hyper-surfaces; that is, the unknown operational mode is assigned to the mode in which the calculated distance is the minimal.

The experimental setup is explained in section 2 and parameter estimation of the frame model along with the feature vector representation of the system is given in details in section 3. In section 4, hyper-surface construction and fault isolation of the system are presented. Finally, the results and discussion are presented in section 5, and conclusion is explained in chapters 6.

2. Experimental Setup

The experimental setup of the laboratory-scale frame structure and its schematic view are shown in Fig's. **1-2**, respectively

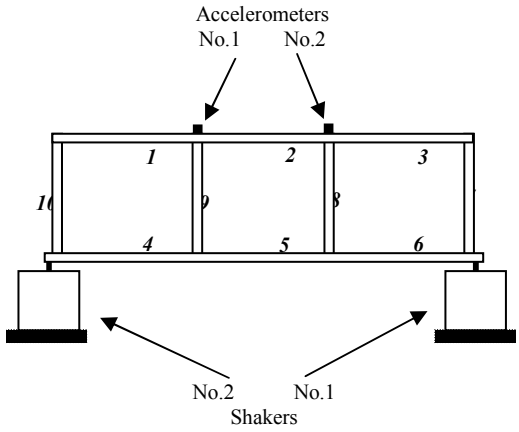

Fig. (1): Schematic drawing of the frame experimental setup.

Fig. (2): The experimental setup of the frame structure.

As shown in the figure, the frame has 10 elements and 2 supports and its members have been made from $20\times20\ mm$ steel hollow section of which length is 300_{mm}. The frame has been mounted on two shakers which are excited by support forces exerted from the shakers. Tests have been done by the PULSE™ system.

During each test, the data was recorded for 20 seconds with the sampling frequency of F*s*=256 Hz. Tests of one input and/or two inputs were performed by exciting one or two shakers. The shaker which was off in the one-input test was considered as a spring support. The input signals

were in the form of swept-cosine. Shaker No. 1 swept up to 60 Hz and shaker No. 2 swept up to 50 Hz. The recorded accelerations by the two accelerometers were used as the output signals of the system.

3. Parameters Estimation and Feature Vector Extraction

The parametric modeling and feature vector extraction are explained as follows.

3.1 Parametric Modeling

In parametric modeling, first an appropriate standard input-output model based on the physical nature of the system is selected and the order is chosen by the AIC criterion [21]. It is to be mentioned that in order to make the proposed method practical and realistic, model parameterization (model structure and order) remains fixed during the experiments. A part of the input-output data of the actual system is fed to the selected model, and estimation of parameters is performed, then the obtained model is validated by one-step-ahead prediction by applying that part of data which has not been used in the modeling step. Parametric identification of the frame including modeling and validating will be explained next.

3.1.1 Modeling

One of the major steps in the proposed approach is modeling of the system. As the one-step-ahead prediction results show, an ARX (Auto Regressive with eXogenous input) and VARX (Vector Auto Regressive with eXogenous input) models were appropriate for modeling the frame. It should be mentioned that the proposed method is applicable to any type of parametric models. The ARX and VARX models are represented in the following forms [22]:

$$\sum_{n_a=0}^{4} a_{n_a}.y(t-n_a)=\sum_{n_b=0}^{3} b_{n_b}u(t-n_b)+w(t)\ ;\ a_0=1, \quad (1)$$

$$a_{n_a}.y(t-n_a)= \sum_{n_a=0}^{4}\begin{bmatrix} b_1+b_2q^{-1} & b_3+b_4q^{-1}\end{bmatrix}\begin{bmatrix}u_1(t)\\ u_2(t)\end{bmatrix}+w(t) \quad (2)$$

$$;a_0=1\ ,$$

$$\begin{bmatrix}1+a_1q^{-1}+a_2q^{-2} & 0\\ a_3q^{-1} & 1+a_4q^{-1}\end{bmatrix}\begin{bmatrix}y_1(t)\\ y_2(t)\end{bmatrix}= \begin{bmatrix}b_1+b_2q^{-1}\\ b_3+b_4q^{-1}\end{bmatrix}u(t)+\begin{bmatrix}w_1(t)\\ w_2(t)\end{bmatrix}\ , \quad (3)$$

$$\begin{bmatrix}1+a_1q^{-1}+a_2q^{-2} & 0\\ a_3q^{-1} & 1+a_4q^{-1}\end{bmatrix}\begin{bmatrix}y_1(t)\\ y_2(t)\end{bmatrix}= \begin{bmatrix}b_1 & b_2\\ b_3 & b_4\end{bmatrix}\begin{bmatrix}u_1(t)\\ u_2(t)\end{bmatrix}+\begin{bmatrix}w_1(t)\\ w_2(t)\end{bmatrix}\ , \quad (4)$$

where y, u, and w are output, input, and noise signals, respectively. Also, a and b are coefficients and q^{-1} is the backshift operator which is:

$$q^{-1}y(t)=y(t-1). \quad (5)$$

The first canonical form of the parametric models is used in VARX models and described as follows [23]. The general form of VARX model is:

$$\mathrm{A}(q^{-1})\ Y(t)=\mathrm{B}(q^{-1})\ U(t-k)+W(t), \quad (6)$$

$\mathrm{A}(q^{-1})$ and $\mathrm{B}(q^{-1})$ are matrix polynomials, where $\mathrm{A}(q^{-1})$ in two-output models is as follows:

$$\mathrm{A}(q^{-1})=\begin{bmatrix}A_1(q^{-1}) & A_2(q^{-1})\\ A_3(q^{-1}) & A_4(q^{-1})\end{bmatrix}. \quad (7)$$

The first canonical form is defined that the matrix polynomial $\mathrm{A}(q^{-1})$ obeys the following conditions:

I) $\mathrm{A}(q^{-1})$ is lower triangular (i.e., $A_2(q^{-1})=0$);

II) A(0) = I ; thus:

$$A_1(q^{-1})=1+a_{11}q^{-1}+a_{12}q^{-2}+\cdots+a_{1l}q^{-l}\ ,$$
$$A_3(q^{-1})=a_{31}q^{-1}+a_{32}q^{-2}+\cdots+a_{3g}q^{-g}\ , \quad (8)$$
$$A_4(q^{-1})=1+a_{41}q^{-1}+a_{42}q^{-2}+\cdots+a_{4r}q^{-r}\ ,$$

III) Degree of $A_3(q^{-1})$ $\leq$ degree of $A_4(q^{-1})$ (i.e., $g \leq r$);

IV) $\mathrm{B}(q^{-1})$ is arbitrary.

All the above-mentioned models are written in the following linear regression form:

$$Y(t)=\Phi^{\mathrm{T}}(t)\ \theta+W(t) \quad (9)$$

where, $Y(t)$ and $W(t)$ are the output and noise signals, respectively; in single-output and two-output models, they are:

$$W(t)=w(t)\ ,Y(t)=y(t)\ \text{, and}$$
$$W(t)=\begin{bmatrix}w_1(t)\\ w_2(t)\end{bmatrix}, Y(t)=\begin{bmatrix}y_1(t)\\ y_2(t)\end{bmatrix}\ . \quad (10)$$

The inputs and outputs of the models are chosen to be:

$$MIMO:\begin{cases}u_1=F_1 & u_2=F_2\\ y_1=a_1 & y_2=a_2\end{cases},\ MISO:\begin{cases}u_1=F_1 & u_2=F_2\\ y=a_1\end{cases},$$
$$SIMO:\begin{cases}u=F_1\\ y_1=a_1 & y_2=a_2\end{cases},\ SISO:\begin{cases}u=F_1\\ y=a_1\end{cases}\ . \quad (11)$$

$\vec{F}_1$ and $\vec{F}_2$ are the forces exerted by the shakers 1 and 2, and also $\vec{a}_1$ and $\vec{a}_2$ are the accelerations measured by the accelerometers 1 and 2,

respectively. Also $\Phi(t)$'s which include any type of the above models, are selected to be:

$$\Phi(t)_{SISO} = \begin{bmatrix} y(t-1) \\ y(t-2) \\ y(t-3) \\ y(t-4) \\ u_1(t) \\ u_1(t-1) \\ u_1(t-2) \\ u_1(t-3) \end{bmatrix}, \quad \Phi(t)_{SIMO} = \begin{bmatrix} y_1(t-1) & 0 \\ y_1(t-2) & 0 \\ u_1(t) & 0 \\ u_1(t-1) & 0 \\ 0 & y_1(t-1) \\ 0 & y_2(t-1) \\ 0 & u_1(t) \\ 0 & u_1(t-1) \end{bmatrix}, \tag{12}$$

$$\Phi(t)_{MISO} = \begin{bmatrix} y(t-1) \\ y(t-2) \\ y(t-3) \\ y(t-4) \\ u_1(t) \\ u_1(t-1) \\ u_2(t) \\ u_2(t-1) \end{bmatrix}, \quad \Phi(t)_{MIMO} = \begin{bmatrix} y_1(t-1) & 0 \\ y_1(t-2) & 0 \\ u_1(t) & 0 \\ u_2(t) & 0 \\ 0 & y_1(t-1) \\ 0 & y_2(t-1) \\ 0 & u_1(t) \\ 0 & u_2(t) \end{bmatrix}.$$

The parametric feature vector in all of the above mentioned models is:

$$\theta = [\theta_1 \ \ \theta_2 \ \ \theta_3 \ \ \theta_4 \ \ \theta_5 \ \ \theta_6 \ \ \theta_7 \ \ \theta_8]^{\mathrm{T}}, \tag{13}$$

which consists of 8 entities (four of which correspond to the autoregressive estimated parameters and the remaining four are associated with the exogenous ones). By casting the obtained data from the tests in the linear regression form, the following set of equations are obtained:

$$\begin{cases} Y(1) = \Phi^{\mathrm{T}}(1)\theta + W(1) \\ Y(2) = \Phi^{\mathrm{T}}(2)\theta + W(2) \\ \vdots \\ Y(N) = \Phi^{\mathrm{T}}(N)\theta + W(N) \end{cases} \Rightarrow \tag{14}$$

$$\begin{bmatrix} Y(1) \\ Y(2) \\ \vdots \\ Y(N) \end{bmatrix} = \begin{bmatrix} \Phi^{\mathrm{T}}(1) \\ \Phi^{\mathrm{T}}(2) \\ \vdots \\ \Phi^{\mathrm{T}}(N) \end{bmatrix} \begin{bmatrix} \theta_1 \\ \theta_2 \\ \vdots \\ \theta_8 \end{bmatrix} + \begin{bmatrix} W(1) \\ W(2) \\ \vdots \\ W(N) \end{bmatrix},$$

where, N is the number of measurements (or the number of input-output sets). The compact form of Eq. (14) may be written as:

$$Y = \Phi\ \theta + W, \tag{15}$$

inwhich, the prediction error vector is:

$$W = Y - \Phi\ \theta. \tag{16}$$

Y and Φ for one-output models are an $N \times 1$ vector and an $N \times 8$ matrix and for two-output models are $2N \times 1$ vector, and a $2N \times 8$ matrix, respectively. If the number of measurements in the one-output models is 8, Φ will be a square matrix and if Φ is non-singular, the parameter vector will have a unique answer which is obtained from solving the set of linear Eq. (14). Due to the disturbances and model errors, more data will be used (i.e., $N > 8$). Also, since the first and second rows of Φ in the two-output models have 4 non-zero members, the number of measurements will be more than 4 times (i.e., $N > 4$). Finally, the parameter vector θ in any of SISO, MISO, SIMO, and MIMO models will be obtained by minimizing the prediction errors and the least squares method in the following way [22]:

$$\theta = [\Phi^{\mathrm{T}}\Phi]^{-1}\Phi^{\mathrm{T}}\ Y\ . \tag{17}$$

3.1.2 Validating

In this step, the responses of the frame and parametric models are compared to validate the obtained parametric models. The input signals are shown in Fig. **3**.

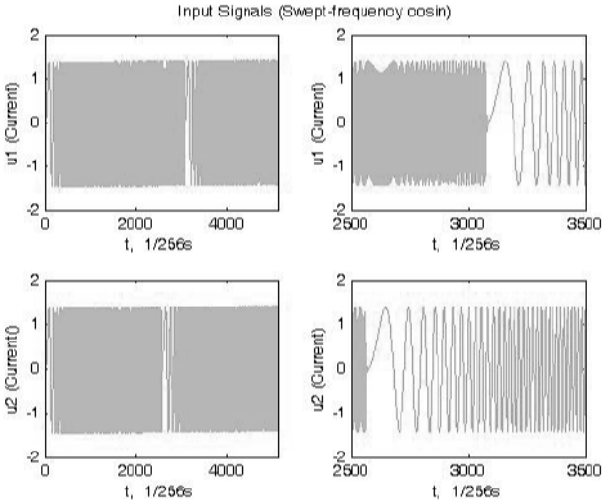

Fig. (3): Input signals.

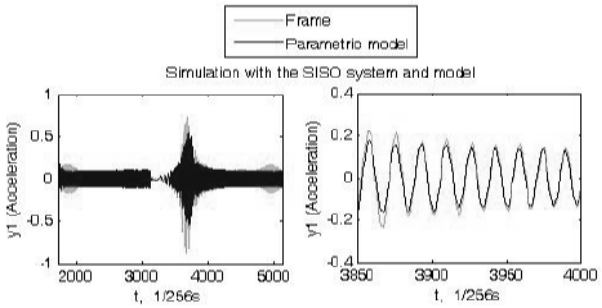

Fig. (4): Single-Input Single-Output responses of model and system

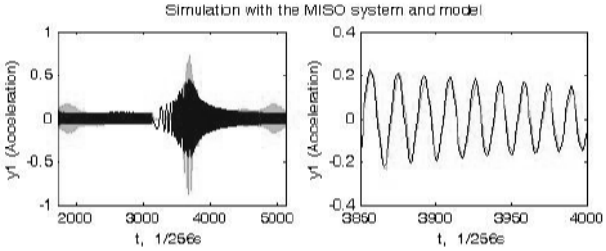

Fig. (5): Two-Input Single-Output responses of model and system.

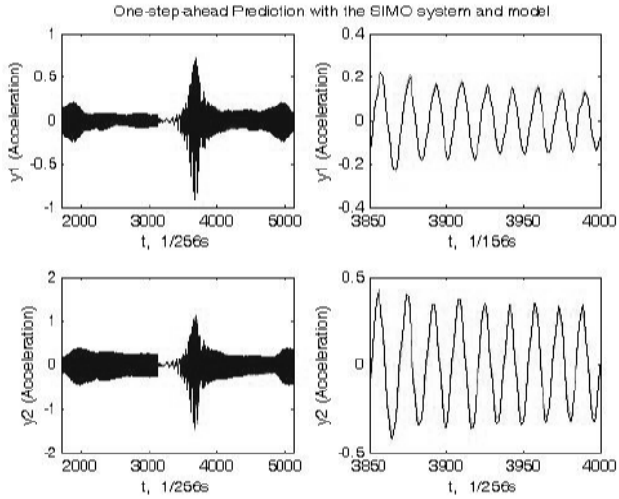

Fig. (6): Single-Input Two-Output responses of model and system.

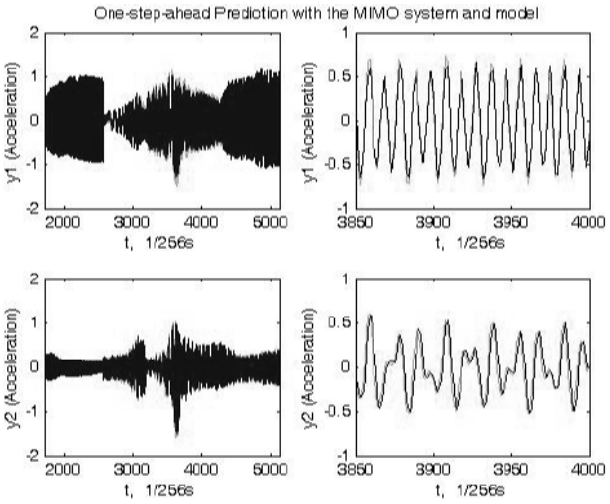

Fig. (7): Two-Input Two-Output responses of model and system.

In order to remove the instabilities of the beginning of the tests, the first 20 data in parameter estimation were not used. Parameter estimation was done by 1700 data (21-1720) and validation was also performed by using 3400 data (1721-5120). For validation, the simulation and one-step-ahead prediction results for SISO, MISO, SIMO, and MIMO models are shown in Fig's. **4 -7**.

3.2 Forming Feature Vector

In different steps of the geometric approach, model parameters were obtained by using all the recorded data (except for the transient zone). Since the comparison of results corresponding to both probabilistic and deterministic spaces is considered in validation, the feature vector θ and the distance function in the two mentioned spaces will be used as follows [24]. In the following the formal definition of the distance function and distance between the two vectors in deterministic and probabilistic senses in our model, are given and then the methodology is extended to the distance between a point and hyper-surface(s).

3.2.1 Deterministic Space and Distance Function

The distance between the two deterministic vectors $\boldsymbol{x} = [x_1 \ \cdots \ x_n]^{\mathrm{T}}$ and $\boldsymbol{y} = [y_1 \ \cdots \ y_n]^{\mathrm{T}}$ in an n-dimensional Euclidean space is:

$$\begin{aligned} d_D^2(\boldsymbol{x},\boldsymbol{y}) &= \|\boldsymbol{x}-\boldsymbol{y}\|^2 \ , \\ &= (\boldsymbol{x}-\boldsymbol{y})^T.(\boldsymbol{x}-\boldsymbol{y}) \ , \\ &= \sum_{i=1}^{n}(x_i - y_i)^2 \ . \end{aligned} \tag{18}$$

In the deterministic space, the members of the feature vector, θ, include only the model parameters. Therefore, in this space, θ and the distance function of two vectors are:

$$\theta = [\mu_\theta]^{\mathrm{T}} = [\theta_1 \quad \theta_2 \quad \ldots \quad \theta_8]^{\mathrm{T}}, \tag{19}$$

$$D(\theta,\theta^{\mu}) = tr[(\mu_\theta - \mu_\theta^{\mu})(\mu_\theta - \mu_\theta^{\mu})^{\mathrm{T}}]. \tag{20}$$

3.2.2 Probabilistic Space and Distance Function

In the probabilistic space, the inner product of two elements, x and y, is defined as:

$$(x \mid y) = E(x.y) \ . \tag{21}$$

Since x and y are linear combinations of random variables with finite variances, their inner product can be calculated from the second-order statistics of the random variables.

For the two scalar random variables x and y:

$$\begin{aligned} (x \mid y) &= E(x.y) \ , \\ (x \mid y) &= \bar{x}.\bar{y} + \sigma_{xy} \ , \end{aligned} \tag{22}$$

where, $\bar{x} = E(x)$ and $\sigma_{xy} = E(\bar{x}.\bar{y})$ are the expectation of x and cross-correlation of the random variables x and y, respectively. Hence, the norm of x, $\|x\|$, may be written as:

$$\|x\| = \sqrt{\bar{x}^2 + \sigma_x^2} \ , \tag{23}$$

and the distance squared between x and y will be:

$$\begin{aligned} d_P^2(x,y) &= \|x-y\|^2 \ , \\ &= E((x-y)^2) \ , \\ &= (\bar{x}-\bar{y})^2 + \sigma_x^2 + \sigma_y^2 - 2\sigma_{xy} \ . \end{aligned} \tag{24}$$

where, σ_x^2 and σ_y^2 are the variances of the random vectors x and y, respectively. However, in practical application to FDI, the cross-correlation between two random variables, σ_{xy}, is not a priori known. The above expression should be thus modified. Denoting as $\overline{d^2}$ the modified d^2, may be written as:

$$\overline{d_P^2(x,y)} = (\bar{x}-\bar{y})^2+\sigma_x^2+\sigma_y^2-2\sigma_x.\sigma_y, \quad (25)$$
$$= (\bar{x}-\bar{y})^2+(\sigma_x-\sigma_y)^2.$$

Notice that when the random vectors x and y are highly correlated the modified distance function is equivalent to the real distance function, which:

$$\overline{d_P(x,y)} = d_P(x,y). \quad (26)$$

Since the norm of the vector x with respect to the Modified Probabilistic space can be decomposed into two components, namely the mean and the variance, hence the modified distance between two random variables has a meaningful geometric representation.

For the two random vectors $\boldsymbol{x}=[x_1 \ \cdots \ x_m]^{\mathrm{T}}$ and $\boldsymbol{y}=[y_1 \ \cdots \ y_m]^{\mathrm{T}}$, the inner product and norm cab are extended as follows:

$$(\boldsymbol{x},\boldsymbol{y}) = Tr(E(\boldsymbol{x}\boldsymbol{y}^T)),$$
$$= Tr[\bar{\boldsymbol{x}}\,\bar{\boldsymbol{y}}^T]+Tr[E((\boldsymbol{x}-\bar{\boldsymbol{x}})(\boldsymbol{y}-\bar{\boldsymbol{y}})^T)], \quad (27)$$
$$= Tr[\bar{\boldsymbol{x}}\,\bar{\boldsymbol{y}}^T]+Tr[\boldsymbol{P}_{xy}],$$

$$\|\boldsymbol{x}\| = Tr(E(\boldsymbol{x}\boldsymbol{x}^T)),$$
$$= Tr[\bar{\boldsymbol{x}}\,\bar{\boldsymbol{x}}^T]+Tr[E((\boldsymbol{x}-\bar{\boldsymbol{x}})(\boldsymbol{x}-\bar{\boldsymbol{x}})^T)], \quad (28)$$
$$= \sum_{i=1}^{m}\bar{x}_i^2+Tr[\boldsymbol{P}_x],$$
$$= \sum_{i=1}^{m}(\bar{x}_i^2+\sigma_{x_i}^2),$$
$$= \boldsymbol{x}_P^T\boldsymbol{x}_P.$$

In the above, $\boldsymbol{x_P}=[\bar{x}_1\cdots\bar{x}_m,\sigma_{x_1}\cdots\sigma_{x_m}]^{\mathrm{T}}$ and $\boldsymbol{y}_P$ is also analogous to $\boldsymbol{x}_P$. $\boldsymbol{P_x}$, $\boldsymbol{P_y}$, and $\boldsymbol{P_{xy}}$ are the covariance matrices of the random vectors $\boldsymbol{x}$, $\boldsymbol{y}$, and their cross-covariance matrix. $Tr[.]$ represents the trace of the indicated matrix. The squared distance between the two random vectors can be easily shown as:

$$d_P^2(\boldsymbol{x},\boldsymbol{y}) = Tr[(\boldsymbol{x}-\bar{\boldsymbol{x}})(\boldsymbol{y}-\bar{\boldsymbol{y}})^T]+Tr[\boldsymbol{P}_x+\boldsymbol{P}_y-2\boldsymbol{P}_{xy}],$$
$$= \sum_{i=1}^{m}(\bar{x}_i-\bar{y}_i)^2+\sum_{i=1}^{m}(\sigma_{x_i}^2+\sigma_{y_i}^2-2\sigma_{x_iy_i}). \quad (29)$$

Also, the modified squared distance will be:

$$\overline{d_P^2(\boldsymbol{x},\boldsymbol{y})} = Tr[(\boldsymbol{x_P}-\boldsymbol{y}_P)(\boldsymbol{x_P}-\boldsymbol{y}_P)^T], \quad (30)$$
$$= [(\boldsymbol{x_P}-\boldsymbol{y}_P)^T(\boldsymbol{x_P}-\boldsymbol{y}_P)].$$

Equation (30) is obtained from Eq. (29) by approximating $\sigma_{x_iy_i}=\sigma_{x_i}\sigma_{y_i}$. Indeed, in the probabilistic space, the members of the feature vector, $\boldsymbol{\theta}$, include the model parameters as well as their variances. Therefore, in this space, $\boldsymbol{\theta}$ and the distance function of two vectors are:

$$\boldsymbol{\theta}=[\mu_\theta\,|\,(diagP_\theta)^{\mathrm{T}}]^{\mathrm{T}}=\left[\theta_1\cdots\theta_8 \ \ \sigma_{\theta_1}^2\cdots\sigma_{\theta_8}^2\right]^{\mathrm{T}}, \quad (31)$$

$$D(\boldsymbol{\theta},\boldsymbol{\theta}')=tr[(\mu_\theta-\mu_\theta')(\mu_\theta-\mu_\theta')^{\mathrm{T}}+(\sigma_\theta^2-\sigma_{\theta'}^2)(\sigma_\theta^2-\sigma_{\theta'}^2)^{\mathrm{T}}]. \quad (32)$$

Parameters' variances which are the diagonal members of the parameters' covariance matrix are obtained as follows [25]:

$$P_\theta := \mathrm{Cov}(\theta)=\lambda_0(\Phi^{\mathrm{T}}\Phi)^{-1}, \quad (33)$$
and $\lambda_0 = mean[(\mathrm{Y}-\Phi\theta)^{\mathrm{T}}(\mathrm{Y}-\Phi\theta)]/(N-12)$.

4. Modeling of Faulty Modes and Fault Detection and Isolation

Consider that the actual fault locus depends upon the number of physical parameters involved in the fault mode. Thus, if a system fault corresponds to only one physical parameter variations (for example, K), the estimated parameters (in the estimated parameter space) will be functions of that parameter only. For instance, in the one-degree-of-freedom example, three estimated parameters change because of changes in only one physical parameter, i.e., stiffness. Since in this study the small to moderate variations are considered, the actual fault locus is a line (hyper-surface) in the 3-dimensional parameter spaces (generally speaking, hyper-space). The crack fault is represented by the variation of the physical parameters K (spring coefficient) and C (damping coefficient), and fault representation will be two lines correspond to the case where only K or C vary. As it may be seen, the hyper-surface associated with the variation of K and C can in this case be well approximated by a hyper-plane.

4.1 Hyper-Planes Construction of the Frame's Fault Modes

Cracks with various severity and locations in members 4, 5, and 6 were considered as three different faulty modes. Then the tests were performed and the related feature vectors were formed. Finally, using the feature vectors in constructing the hyper-plane, modeling of the fault mode was carried out.

For this purpose, three frames were prepared, each of which were used separately for modeling as well as validating the proposed fault isolating method. Testing and recording data of the faulty modes were started when the member had one crack, then by producing another crack, tests and data recordings were repeated This procedure continued until the necessary number of faults in each mode is obtained for hyper-plane construction, which in our case was 33 faults for each member. In order to control the test, and save time, the cracks are

initiated by producing grooves by coping as shown in Fig. **8**.

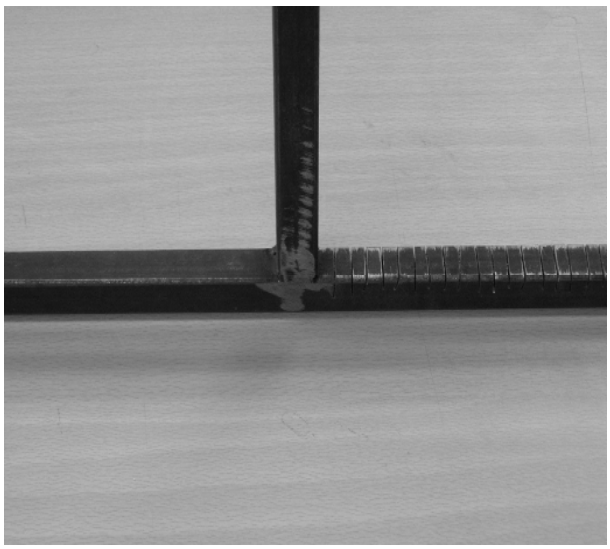

Fig. (8): The cracked frame structure.

The locus of feature vectors corresponds to i^{th} mode $(i=1,2,3)$ is a hyper-plane (i.e., $f^i(\boldsymbol{\theta})=0$). In the deterministic space (i.e., $\boldsymbol{\theta}=[\theta_1 \ \theta_2 \cdots \theta_8]^{\mathrm{T}}$), the equation of the hyper-plane is:

$$\theta_1+\theta_2\alpha_1^i+\theta_3\alpha_2^i+\cdots+\theta_8\alpha_7^i+\alpha_0^i=0 \ ; i=1,2,3, \quad (34)$$

where, α_j^i $(j=0,1,2,\ldots,7)$ are the hyper-plane's coefficients, that is, the normal vector n^i, representing the i[th] hyper-plane is:

$$n^i=[1 \ \alpha_1^i \ \alpha_2^i \ \cdots \ \alpha_7^i]^{\mathrm{T}}. \quad (35)$$

The system of equations to obtain the hyper-plane's coefficients will be:

$$f^i(\boldsymbol{\theta})=(n^i)^{\mathrm{T}}\boldsymbol{\theta}+\alpha_0^i=0. \quad (36)$$

Any of the feature vectors obtained from a specific member fault related to the i^{th} mode should yield the equation of the i^{th} hyper-plane $(f^i(\boldsymbol{\theta})=0)$. Therefore, by replacing the parameters from N faults related to the i^{th} mode in Eq. (34), N equations will be obtained by which the hyper-plane coefficients can be estimated. Considering the stochastic properties of the system and to estimate the hyper-plane coefficients properly, the number of equations is considered to be over two times of the number of hyper-plane coefficients [26]. As in Eq. (19), the members of the feature vector in the deterministic space are the same as the model parameters i.e. the number of the hyper-plane coefficients is the same as the number of model parameters. Therefore, in order to estimate the hyper-plane coefficients properly, the parameters of $17(2\times8+1)$ different faults of each mode were used and consequently the following system of equations have been obtained:

$$\begin{aligned}
&\theta_1^{i\,1}+\theta_2^{i\,1}\alpha_1^i+\theta_3^{i\,1}\alpha_2^i+\cdots+\theta_8^{i\,1}\alpha_7^i+\alpha_0^i=0 \ ,\\
&\theta_1^{i\,2}+\theta_2^{i\,2}\alpha_1^i+\theta_3^{i\,2}\alpha_2^i+\cdots+\theta_8^{i\,2}\alpha_7^i+\alpha_0^i=0 \ , \quad (37)\\
&\vdots \quad \vdots \quad \vdots \quad \vdots \quad \vdots \quad \vdots\\
&\theta_1^{i\,17}+\theta_2^{i\,17}\alpha_1^i+\theta_3^{i\,17}\alpha_2^i+\cdots+\theta_8^{i\,17}\alpha_7^i+\alpha_0^i=0 \ .
\end{aligned}$$

To estimate the hyper-plane's coefficients, the above-mentioned system of equations is in the form of linear regression as:

$$\begin{bmatrix} 1 & \theta_2^{i\,1} & \theta_3^{i\,1} & \cdots & \theta_8^{i\,1} \\ 1 & \theta_2^{i\,2} & \theta_3^{i\,2} & \cdots & \theta_8^{i\,2} \\ \vdots & \vdots & \vdots & & \vdots \\ 1 & \theta_2^{i\,17} & \theta_3^{i\,17} & \cdots & \theta_8^{i\,17} \end{bmatrix} \begin{bmatrix} \alpha_0^i \\ \alpha_1^i \\ \vdots \\ \alpha_7^i \end{bmatrix} = - \begin{bmatrix} \theta_1^{i\,1} \\ \theta_1^{i\,2} \\ \vdots \\ \theta_1^{i\,17} \end{bmatrix}, \quad (38)$$

or, in the compact form:

$$\psi^i\alpha^i=-\mathrm{a}_1^i, \quad (39)$$

where, α^i and ψ^i are a 8×1 vector and a 17×8 matrices, respectively. The hyper-plane's coefficients vectors were estimated by the least squares method as follows[26]:

$$\alpha^i=[(\psi^i)^{\mathrm{T}}\psi^i]^{-1}(\psi^i)^{\mathrm{T}}(-\mathrm{a}_1^i). \quad (40)$$

Estimating the hyper-plane coefficients in the probabilistic space were performed in the similar way, but according to Eq. (31) the members of the feature vector in the probabilistic space include parameters variances as well as model parameters i.e., the number of the hyper-plane coefficients is twice as much as the number of model parameters. Therefore, in order to estimate the hyper-plane coefficients properly, the parameters of 33 $(2\times16+1)$ different faults of each mode were used.

4.2 Fault Detection and Isolation

Occurrence of a crack was considered as a fault, whereas the presence of crack(s) in any of the members 4, 5, or 6 was regarded as a faulty mode. By creating 1 to 39 cracks in each of the members, and performing of tests by frame shaking, the data of 39 different faults for each of the aforementioned members were recorded and the data of 33 situations for modeling the faulty mode (in the probabilistic space) and the data of remaining situations (6 situations) were used as unknown operational modes which were tiny, moderate and sever faults. It is necessary to mention that modeling the faulty modes in the deterministic space was performed by using the data obtained from 17 situations. It should be noticed that the data used in the unknown operational modes were not used for modeling the faulty modes. Considering 6 unknown operational modes in each of the three

members, 18 unknown operational modes for fault isolation were done all together. For fault isolation, the distance between feature vector of the unknown operational mode θ^{u}, and each of the hyper-planes corresponding to the faulty modes are calculated by minimizing the distance between vector θ^{u} to vector θ associated with each hyper-plane (minimizing the distance function is subject to the hyper-plane equation $f^{i}(\theta)=0$).

In order to increase the computational efficiency and noting that the distance function is always non-negative, the quadratic form of the distance function was minimized. To convert the constrained minimization to an unconstrained optimization, the Lagrange Multipliers approach is adopted [27]. The Lagrangian is obtained by using the Lagrange Multipliers and the distance function as follows:

$$\begin{aligned} L &= d^{2}(\theta^{u},\theta)+\gamma f^{i}(\theta) \\ &= (\theta^{u}-\theta)(\theta^{u}-\theta)^{\mathrm{T}}+\gamma((n^{i})\theta+\alpha_{0}^{i}), \end{aligned} \tag{41}$$

where, γ and $d(\theta^{u},\theta)$ are the Lagrange multiplier and the distance between vector θ^{u} and vectors θ, respectively. Optimizing L is equivalent to minimizing the distance function which is subject to the hyper-plane equation. The optimizing L and forming the following equations are performed by differentiation of L with respect to θ and γ:

$$\begin{cases} \dfrac{\partial L}{\partial \theta}=0 \\ \dfrac{\partial L}{\partial \gamma}=0 \end{cases}, \tag{42}$$

Therefore, a set of $1+8$ linear equations in the deterministic space and a set of $1+16$ linear equations in the probabilistic space were obtained and rewritten in the following form and by solving them a θ was obtained, in which the Lagrangian is optimal, i.e. the amount of the distance function is minimal:

$$\begin{bmatrix} I & n^{i} \\ (n^{i})^{\mathrm{T}} & 0 \end{bmatrix}\begin{bmatrix} \theta \\ \gamma \end{bmatrix}=\begin{bmatrix} \theta^{u} \\ -\alpha_{0}^{i} \end{bmatrix}, \tag{43}$$

where, I is an 8×8 identity matrix in the deterministic space and a 16×16 identity matrix in the probabilistic space. Considering Eqs. (41) and (42), minimization of L includes the hyper-plane equation $f^{i}(\theta)=0$, and the minimum distance of θ^{u} to θs related to the aforementioned hyper-plane. So, the distance between vector θ^{u} and the hyper-plane $f^{i}(\theta)=0$ which is the optimal of L is obtained by solving Eq. (43) in the following way:

$$\begin{aligned} d(\theta^{u},f^{i}(\theta)) &= Min \;\; d(\theta^{u},\theta) \;\; ; \;\; \theta\in f^{i}(\theta), \\ &= n^{i}[(n^{i})^{\mathrm{T}}n^{i}]^{-1}[(n^{i})^{\mathrm{T}}\theta^{u}+\alpha_{0}^{i}] \;. \end{aligned} \tag{44}$$

By repeating the above-mentioned procedure for each one of the operational modes, the distances between the vector θ^{u} and the hyper-planes were obtained. Finally these calculated distances are compared with each other and the unknown operational mode is classified as the mode with which the calculated distance is the minimum. That is:

$$\begin{aligned} &d(\theta^{u},f^{i}(\theta))<d(\theta^{u},f^{j}(\theta)) \qquad \forall i\neq j \;\; ; \;\; i,j=1,2,3 \;, \\ &\theta^{u}\in f^{i}(\theta) \;. \end{aligned} \tag{45}$$

5. Results and Discussion

In this study two test sets, Set 1 with single input and two outputs, and Set 2 with two inputs and two outputs were carried out. The input-output signals from both set of the tests were recorded.

Set 1 consists of the two SISO and SIMO subsets, and Set 2 includes the two MISO and MIMO subsets.

For fault isolation, the distances of the feature vectors of the unknown operational modes to any of the faulty mode hyper-planes have been calculated. For example, the calculated distances in the probabilistic and deterministic spaces between the points of unknown operational modes and the faulty mode hyper-planes are presented in the form of MIMO system in the table **1**. In this table, every line represents the distances of the feature vector of an unknown operational mode from the faulty mode hyper-planes. The minimum quantity in each line is bold typed, and the minimum quantity is underlined if it does not specify the correct answer.

As it is seen, the results of the frame's fault isolation in the form of MIMO system in the probabilistic space is free from errors, in other words, the minimum distance in all lines is related to the hyper-plane corresponding to the faulty member. Also, 15 correct and 3 wrong answers were obtained after performing (fault isolation) 18 times of the frame in the MIMO system in the deterministic space.

Like the above-mentioned procedure, fault diagnoses of the frame were done by using one or two inputs and one or two outputs. The number and the percentage of the fault isolation errors of the frame in the forms of SISO, MISO, SIMO, and MIMO systems are presented in table **2**.

Table (1): Results of fault isolation of the frame in the form of MIMO system .

Faults	Test Number	Probabilistic Distance from Hyper-plane			Deterministic Distance from Hyper-plane		
		F_1	F_2	F_3	F_1	F_2	F_3
F_1: Faulty Member4	1	**2.3005e-012**	1.6217e-011	1.0130e-011	**2.3200e-004**	2.3093e-003	5.5144e-003
	2	**1.3354e-012**	1.5400e-011	9.5453e-012	**2.3142e-004**	2.0608e-003	5.3362e-003
	3	**1.1065e-012**	1.8687e-011	3.2483e-012	**4.3686e-004**	8.4591e-004	7.6335e-003
	4	**1.9306e-014**	2.1404e-011	3.1408e-012	**2.8688e-005**	4.2582e-005	8.3421e-003
	5	**8.4340e-013**	1.8475e-011	6.8764e-012	**4.4380e-004**	2.2077e-003	1.1217e-002
	6	**2.3736e-012**	1.7502e-011	6.0147e-012	**2.5976e-004**	1.3218e-003	8.7209e-003
F_2: Faulty Member5	7	3.4241e-011	**4.1363e-013**	3.6151e-012	7.6126e-004	**9.7586e-005**	7.1209e-003
	8	3.0898e-011	**3.6468e-014**	2.0231e-013	**4.0388e-004**	8.3286e-004	2.5229e-003
	9	4.2078e-011	**2.1039e-013**	2.0450e-012	1.8003e-003	**3.0373e-004**	5.1797e-003
	10	3.5401e-011	**6.7073e-014**	3.0478e-012	7.2743e-004	**4.8334e-004**	1.3036e-003
	11	4.6462e-011	**1.5614e-013**	9.2019e-013	1.6897e-003	**8.9704e-004**	4.9601e-003
	12	4.0829e-011	**8.3354e-013**	1.9650e-012	2.1886e-003	**2.2853e-004**	4.7232e-003
F_3: Faulty Member6	13	2.8930e-011	1.1257e-011	**1.5490e-012**	4.4344e-003	2.1099e-003	**1.1869e-005**
	14	1.2642e-010	3.2231e-011	**7.2291e-013**	1.3698e-002	1.2593e-003	**2.1204e-004**
	15	1.8278e-011	8.8013e-012	**5.9336e-013**	2.1170e-003	5.6053e-004	**3.7282e-004**
	16	1.0577e-011	7.4291e-012	**1.6345e-012**	4.4330e-004	**2.1853e-004**	1.6509e-003
	17	2.3523e-011	1.0914e-011	**9.8662e-013**	3.3998e-003	1.1876e-003	**2.6274e-004**
	18	8.0376e-012	3.2702e-012	**2.8031e-012**	**1.7846e-003**	2.8420e-003	3.4080e-003

Table (2): Number and percentage of the fault isolation errors.

Space \ System		MIMO	MISO	SIMO	SISO
Probabillistic	Quantity	**0**	**2**	**1**	**4**
	Percent	**0%**	**11.11%**	**5.56%**	**22.22%**
Deterministic	Quantity	**3**	**3**	**4**	**5**
	Percent	**16.68%**	**16.68%**	**22.22%**	**27.78%**

As it is considered, fault diagnoses of the frame in the forms of MIMO and SISO systems have the highest and lowest performance, respectively; this results are compared and shown in Fig. **9**.

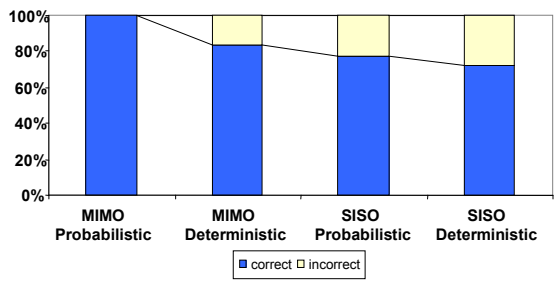

Fig. (9): Results of fault isolation in MIMO and SISO frame.

The above results show that increasing the number of inputs improves the fault isolation performance; as classification error in MIMO model is less than SIMO one, and in MISO model less than the SISO one. The reason is the outputs' further enrichment which is caused by further activation of the system dynamics caused by increasing the number of inputs.

Also, fault isolation scheme in two-output models performs better compared the single-output ones; as classification error in MIMO model is less than MISO one, and in SIMO model less than the SISO one. The reason is to acquire further information on the system dynamics through increasing the number of outputs, while the parametric system identification in two-output models can be done by using less measurement $(N>4)$ than single-output models $(N>8)$.

By using probabilistic space in calculating of the distances and utilizing variances of the estimated parameters in addition to the parameters themselves, the FDI performance noticeably improved in comparison with the deterministic one. Fig. **10** compares the rate of errors of fault isolation in SISO, MISO, SIMO, and MIMO systems.

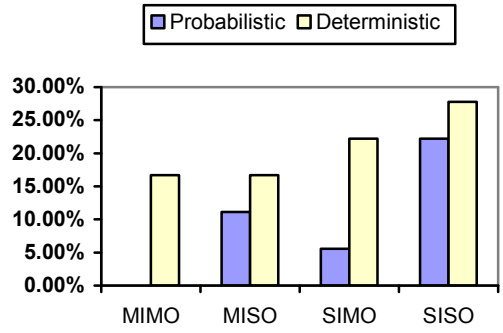

Fig. (10): Fault isolation errors in the probabilistic and deterministic spaces.

In addition, the experimental results and the obtained results from simulation by a finite element model of the frame mentioned in Ref. [19] are compared in table **3** as follows:

Table (3): Percentage of the fault isolation errors in experimental and simulation tests.

Space \ System		MIMO	MISO	SIMO	SISO
Probabillistic	Simulation	**5.81%**	**7.51%**	**7.78%**	**8.49%**
	Experimental	**0%**	**11.11%**	**5.56%**	**22.22%**
Deterministic	Simulation	**8.51%**	**30.60%**	**18.11%**	**28.49%**
	Experimental	**16.68%**	**16.68%**	**22.22%**	**27.78%**

The comparison between experimental and simulation results in the above table shows the agreement of the experimental results.

6. Conclusion

Fault isolation in a frame was performed successfully through the proposed geometric approach. The best performance of fault isolation scheme was obtained for MIMO case. Moreover, in all SISO, MISO, SIMO, and MIMO cases, the probabilistic distance function out formed the deterministic one. The least performance of fault isolation was obtained for SISO case and deterministic space with about 28% classification errors. A any way, increasing the number of input or output measurements improve the proposed method's performance.

Acknowledgement

The tests mentioned in this paper have been done in the Modal Analysis Research Laboratory of Mechanical Engineering Department in Tehran University. I should appreciate that laboratory staff's warm cooperation, especially Mr. Shervin Shahsavari's.

References

1-Willsky, A. S., "A Survey of Design Methods for Failure Detection in Dynamic System", Automatica, Vol. 12, No. 6, pp. 601-611, 1976.

2-Gilmore, J. and McKern, R., "A Redundant Strap-down Inertial Systems Mechanization", Presented at AIAA Guidance, Control, and Flight Mechanics Conf., Santa Barbara, CA, pp. 17-19, Aug. 1970.

3-Tokatli, F., Cinar, A., and Schlesser, J.E., "HACCP with Multivariate Process Monitoring and Fault Diagnosis Techniques: Application to a Food Pasteurization Process", Food Control, Vol. 16, No. 5, pp. 411-422, 2005.

4-Lyde, T.L. and Zimmerman, D.C., "Sensor Failure Detection and Isolation in Flexible Structure, Using System Realization Redundancy", AIAA J. Guidance, Control, and Dynamics, Vol. 16, No. 3, pp. 490-497, 1993.

5-Frisk, E., Aslund, J., "Lower Orders of Derivatives in Non-linear Residual Generation using Realization Theory", Automatica, Vol. 41, No. 10, pp. 1799-1807, 2005.

6-Weihua, Li and Sirish, L.Sh., "Structured Residual Vector-based Approach to Sensor Fault Detection and Isolation", J. Process Control, Vol. 12, No. 3, pp. 429-443, 2002.

7-Zhengang H., Weihua, L., and Sirish L.S., "Fault Detection and Isolation in the Presence of Process Uncertainties", Control Eng. Practice, Vol. 13, No. 5, pp. 587-599, 2005.

8- Sadeghi, M.H. and Fassois, S.D., "Geometric Approach to Failure Identification in Stochastic Dynamical Systems," Ph.D. Dissertation, Mech. Eng. Dep't., Univ. of Michigan, Ann Arbor, 1994.

9-Boukhris, A., Giuliani, S., and Mourot, G., "Rainfall-Runoff Multi-Modelling for Sensor Fault Diagnosis", Control Eng. Practice, Vol. 9, No. 6, pp. 659-671, 2001.

10-Watanabe, K., Yoshimura, T., and Soeda, T.A., "A Diagnosis Method for Linear Stochastic Systems with Parametric Failures", ASME J. Dynamic Systems, Measurement and Control, Vol. 103, No. 1, pp. 28-35, 1981.

11-Basseville, M.A., Benveniste, A., Moustakides, G.V., and Rougee, A., "Detection and Diagnosis of Abrupt Changes in Modal Characteristics of Nonstationary Digital Signals", IEEE Transaction on Information Theory, Vol. 32, No. 3, pp. 412-417, 1986.

12-Isermann, R., "Fault Diagnosis of Machines via Parameter Estimation and Knowwledge Processing", Automatica, Vol. 29, No. 4, pp. 815-835, 1991.

13-Bachschmid, N., Pennacchi, T., and Venia, A., "Identification of Multiple Faults in Rotor

Systems", J. Sound and Vibration, Vol. 254, No. 2, pp. 327-366, 2002.

۱۴- همایون صادقی، م. و رحیمی، ن.، "مدل‌سازی یک موتور سوخت مایع با بکارگیری روش‌های پارامتری شناسایی سیستم"، پانزدهمین کنفرانس سالانه (بین المللی) مهندسی مکانیک، دانشگاه صنعتی امیرکبیر، ۱۳۸۶.

15-Gersch, W., Brotherton, and T., Braun, S., "Nearest Neighbor Time Series Analysis Classification of Faults in Rotating Machinary", ASME J. Vibration, Acoustics, Stress, and Reliability in Design, Vol. 105, No. 2, pp. 178-184, 1983.

16-Sadeghi, M.H. and Fassois, S.D., "Geometric Approach to Nondestructive Identification of Faults in Stochastic Structural Systems", AIAA J., Vol. 35, No. 4, pp. 700-705, 1997.

17-Sakellariou J.S. and Fassois S.D., "Parametric Output Error Based Identification and Fault Detection in Structures Under Earthquake Excitation", European COST F3 Conf. on System Identification and Structural Health Monitoring, Madrid, Spain, pp. 323-332, 2000.

18- Sadeghi, M.H., "Failure Detection and Isolation in a Liquid Propellant Engine", Technical Report of Shahid Hemat Group, 2003.

19-Rahimi, N., Sadeghi, M.H., and Mahjoob, M.J. "Performance of the Geometric Approach to Fault Detection and Isolation in SISO, MISO, SIMO and MIMO Systems", J. Zhejiang Univ. SCIENCE A, Vol. 8, No.9, pp. 1443-1451, Sep. 2007.

۲۰- رحیمی، ن.، همایون صادقی، م. و محجوب، م.، "آشکارسازی و جداسازی عیب در چرخدنده به روش هندسی با استفاده از ورودی و خروجی‌های چندگانه"، شانزدهمین کنفرانس سالانه(بین المللی) مهندسی مکانیک، دانشگاه شهید باهنر کرمان، ۱۳۸۷.

21-Schwartz, G., "Estimating the Dimension of a Model", Annals of Statistics, Vol. 6, No. 1, pp. 461-464, 1987.

22-Soderstrom, T. and Stoica, P., "System Identification", Prentice Hall, U.K., 1989.

23-Kashyap, R.L., and Rao, A.R., "Dynamic Stochastic Models from Empirical Data", Academic Press, New York, 1976.

24-Luenberger, D., "Optimization by Vector Space Method", Wiley, 1986.

25-Ljung, L., "System Identification Theory for the User", Prentice Hall, 2nd Ed., New Jersey, 1999.

26-Myers, R.H., "Classical and Modern Regression with Applications", Duxbury Advanced Series 213-221, 1990.

27-Strang, G. "Introduction to Applied Mathematics", Wellsley, Mass., Wellsley-Camridge Press, 1986.